Materials Transactions, Vol. 46, No. 10 (2005) pp. 2176 to 2179

Characterization of Electroplated Platinum–Iridium Alloys on the Nickel-Base Single Crystal Superalloy

Yingna Wu*, Aya Suzuki, Hideyuki Murakami and Seiji Kuroda

Thermal Spray Group, Materials Engineering Laboratory, National Institute for Materials Science (NIMS), Tsukuba 305-0047, Japan

As a high temperature protective layer, platinum–iridium alloys were electroplated on the nickel-base single crystal superalloy TMS-82+ from amidosulfuric acid solutions by the direct current method. It was found that Ir content in the films was always lower than the ratio of concentration ($[Ir^{3+}]/([PtCl_6^{2-}] + [Ir^{3+}])$) in the electrolytes, indicating that preferential deposition of Pt occurred in this study. The as-deposited Pt–Ir films formed an fcc single phase structure with a granular surface. When Ir content exceeded 3 at%, Pt–Ir films exhibited the ⟨111⟩ preferred growth orientation. It was also found that pre-deposition of Ni and Pt promoted the deposition rate and changed composition of overlaying Pt–Ir films.

(Received April 26, 2005; Accepted August 1, 2005; Published October 15, 2005)

Keywords: *electroplating, direct current method, platinum–iridium films, pre-deposition, Ni-base superalloy*

1. Introduction

Pt-modified aluminide coatings were firstly proposed in the early 1960's[1] and have successfully been deposited as the protective layers on high temperature components since the early 1970's.[2] The utilization of Pt-modified aluminide coatings as bond coat materials for thermal barrier coatings (TBCs) was firstly mentioned in 1993.[3] This type of bond coats is normally produced by initially electrodepositing a platinum layer followed by a diffusion treatment and/or an aluminizing treatment performed through the pack cementation or chemical vapor deposition (CVD) process.[4] The outer layer of the Pt-modified aluminide coatings consists of one of intermetallic phases $PtAl_2$, Pt_2Al_3, $PtAl$[5] or platinum in the solid solution, depending on the deposition parameters. The $PtAl_2$ phase provides an aluminum reservoir but it also deteriorates the mechanical properties of the coatings and embrittles the superalloy/top coat interface.[6] Moreover, the high price of platinum limits its industrial use.

Recently, other platinum group metal (PGM) additions are tried to replace platinum, such as palladium,[7] rhodium[8] and iridium.[9] Iridium has the highest melting temperature (2716 K) among PGMs, high tensile strength (440 MPa) at room temperature,[10] excellent chemical stability, low oxygen permeability, superior hardness and low electrical resistivity. Compared to platinum, iridium has the advantage in terms of its price. In addition, IrAl intermetallics have been found to have potential as alumina formers.[11]

In our group, Ir-aluminide[12,13] and Ir-Ta modified aluminide coatings,[14] deposited through magnetron sputtering, electron beam physical vapor deposition (EB-PVD) or electroplating followed by aluminizing, have been evaluated in terms of their microstructure, mechanical properties and oxidation behaviors. In the present study, Pt–Ir, Pt/Pt–Ir and Ni/Pt–Ir systems were prepared through electrodeposition. The chemical composition, surface morphology and phase identification of Pt–Ir films were investigated. Effects of Ni and Pt pre-deposition on characteristics of electroplated Pt–Ir alloys were also discussed.

*Corresponding author, E-mail: WU.Yingna@nims.go.jp

2. Experimental

Substrate coupons, 25 mm in diameter and 2 mm in thickness, were cut from the nickel-base single crystal superalloy TMS-82+ bar, whose chemical composition consists of Co: 7.7; Cr: 4.5; Mo: 1.8; W: 8.6; Re: 2.5; Al: 5.3; Ta: 6.4; Hf: 0.14; Ni: Bal. (mass%). Before electroplating, samples were mechanically polished with SiC paper up to #600 and degreased with acetone for 10 min in an ultrasonic bath. They were then thoroughly cleaned with NaOH solution (1 mol/L) for 3 min and HCl solution (1 mol/L) for 30 seconds in an ultrasonic bath.

For electroplating Pt–Ir films (3–5 μm in thickness), electrolytes were made from $IrCl_3 \cdot nH_2O$ (supplied by Furuya Metals Co., Ltd., Japan, purity: 99.95 mass%, Ir content: 53.47 mass%) and Pt (supplied by Furuya Metals Co., Ltd., Japan, purity: 99.98 mass%) powders. $IrCl_3 \cdot nH_2O$ was dissolved in HCl solution with heated at 60°C for 30 min. Pt was dissolved in the mixture of HCl and HNO_3 ($HCl:HNO_3 = 3:1$) with heated at 150°C for 30 min. These solutions were mixed with various volume ratio so that various mole fraction of Ir ($[Ir^{3+}]/([PtCl_6^{2-}] + [Ir^{3+}])$) was obtained. Then, NH_2SO_3H was added to the mixture as the complex-forming additives. Typical electrolytes consisted of $[PtCl_6^{2-}] + [Ir^{3+}]$: 0.05 mol/L, NH_2SO_3H: 0.35 mol/L, HCl: 0.010–0.019 mol/L, HNO_3: 0.0004–0.0028 mol/L.

All the solutions were prepared using distilled water and reagent grade chemicals. The electrolyte was filled in a 500 ml beaker with stirring. In order to keep the pH value (2–3), small amount of HCl (1 mol/L) and/or NaOH (1 mol/L) were added during electroplating. Two Ti plates covered with Pt were used as the counter anodes whose surface area is twice as large as that of the sample cathode. The distance between the cathode and anode was 3–5 cm.

In order to investigate the effect of surface composition on the characteristics of electroplated films, pre-electroplating of Pt and Ni was attempted prior to the Pt–Ir electro-

Table 1 Electroplating conditions for Pt–Ir alloys and pre-deposition of Pt and Ni.

Films	Temp. (°C)	pH	C.D. (A/dm^2)	Time (h)
Pt–Ir	80–85	2–3	0.2–2	0.5–4
Pt	55–65	0.5–1	1–2	0.08–0.20
Ni	50–60	4–5	1–2	0.08–0.20

deposition. The PTP-H solution (Nissin Kasei Co., Ltd., Japan) and the Watts nickel bath ($NiSO_4 \cdot 6H_2O$: 0.95 mol/L; $NiCl_2 \cdot 6H_2O$: 0.17 mol/L; H_3BO_3: 0.65 mol/L) were used for the Pt and Ni pre-deposition, respectively. Thickness of the pre-deposited layer was 0.1–0.2 μm. Electroplating conditions are shown in Table 1.

Chemical composition of films was measured by X-ray fluorescence spectrometry (XRF). Crystal structures of deposited films were identified by an X-ray diffractometer (RINT-2500, Rigaku Co., Japan, XRD). Surface and cross-sectional morphologies and element concentration profiles along the cross section of the films were analyzed by a field-emission scanning electron microscope (JSM-6500, JEOL Co., Japan), equipped with an X-ray energy-dispersive spectrometer.

3. Results and Discussion

3.1 Film composition

Figure 1 shows the relationship between Ir ion mole fraction against the total metal ion content ($[Ir^{3+}]/([PtCl_6^{2-}] + [Ir^{3+}])$) in the electrolyte and Ir content in the deposited films. Ir content in the films was always lower than Ir mole fraction. For example, Ir content in the films was only 47 at% even when $[Ir^{3+}]/([PtCl_6^{2-}] + [Ir^{3+}])$ reached 0.95.

It should be noted that these results in film composition did not agree with those in the previous research.[15] It is reported that manufacturing process of iridium chloride salts drastically affected the efficiency of Ir electrodeposition, probably due to the amount of contamination.[16] It is thus speculated that different impurity level in the iridium chloride salts may have altered the results. However, further investigation is required to elucidate it.

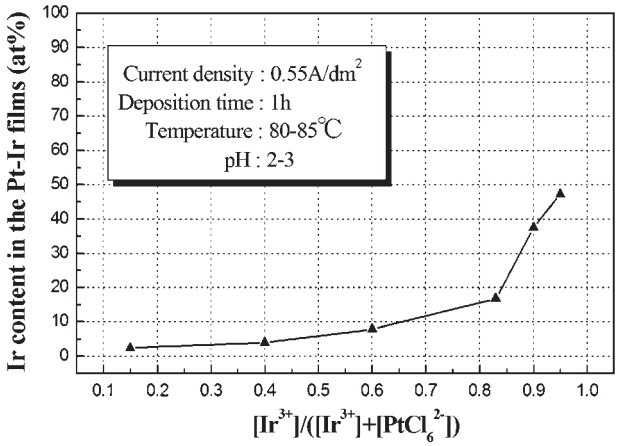

Fig. 1 Relationship between Ir ion mole fraction ($[Ir^{3+}]/([PtCl_6^{2-}] + [Ir^{3+}])$) in the electrolytes and Ir content in the Pt–Ir films.

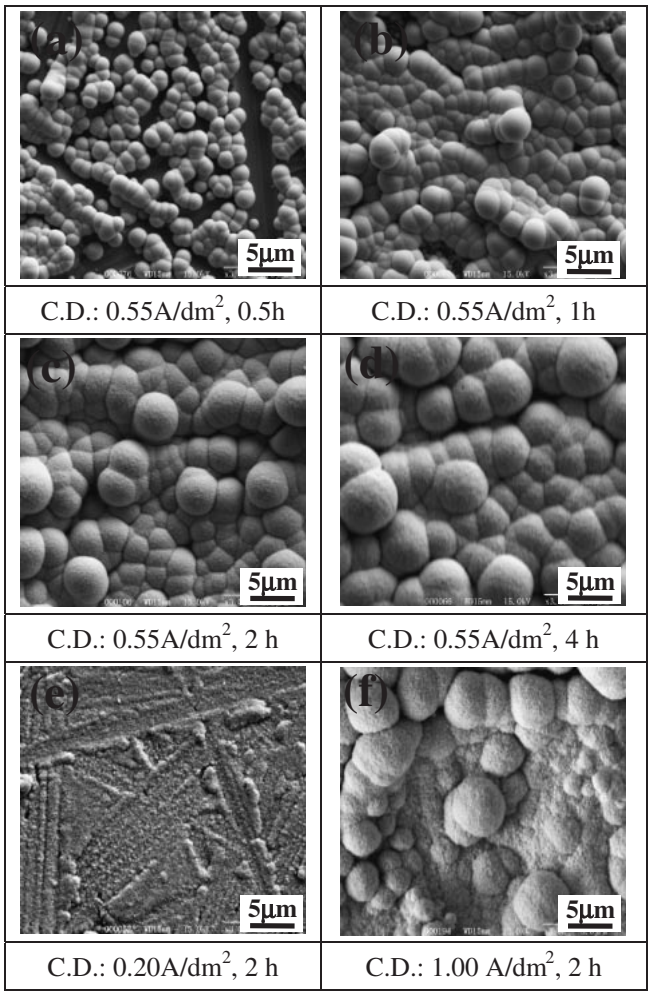

Fig. 2 Surface morphologies of Pt–Ir films at different current density and deposition time ($[Ir^{3+}]/([PtCl_6^{2-}] + [Ir^{3+}]) = 0.95$).

3.2 Surface morphology

In this section, the constant Ir mole fraction (0.95) was chosen. The change in surface morphology as a function of time at the current density (C.D.) of 0.55 A/dm^2 was observed by SEM [Figs. 2(a)–(d)]. It was found that the surface of deposited films was granular, consisting of nodules with various sizes. In the initial stage (within 1 h), the deposits showed discontinuous nodules [Figs. 2(a)(b)]. Increase in film thickness at this stage is mainly due to the growth of these nodules. Then a continuous granular film formed after 2 h [Figs. 2(c)(d)]. As soon as the continuous nodules covered the surface, the growth rate of films slowed down.

Under the same deposition time (2 h), the mean size of nodules increased with the increase in current density [Figs. 2(c)(e)(f)]. At the current density of 0.20 A/dm^2, a smooth film with very fine nodules was formed [Fig. 2(e)], which indicated the very slow growth rate.

3.3 Phase identification

Figure 3 shows the X-ray diffraction patterns of electro-

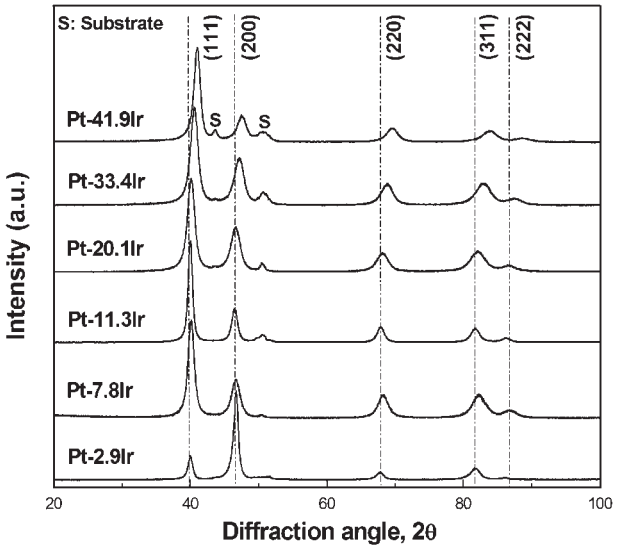

Fig. 3 X-ray diffraction patterns of Pt–Ir films with different Ir content (current density: 0.55 A/dm^2, deposition time: 1 h).

plated Pt–Ir films with various Ir contents. According to the equilibrium phase diagram, Pt and Ir should form a continuous solid solution at high temperatures and a miscibility gap should appear at low temperatures.[17] However, all the profiles indicated the single phase fcc structure, except for the peaks from substrates, although the films were electroplated at 80–85°C. With the increase in Ir content, the diffracted peaks shifted towards the higher angles, indicating that the lattice parameter decreases with increasing Ir content.

It was found that the intensity in the (200) diffraction peak was higher than the standard powder diffraction pattern when the Ir content was below 3 at%, indicating that the preferred orientation changed and the films were highly textured along ⟨200⟩ direction. Since {111} faces correspond to the most densely packed planes with the lowest energy for the fcc structure,[18] most of the grains in the electroplated Pt/Pt–Ir films preferred to be oriented along ⟨111⟩ directions. In the case of Ir < 3 at%, on the other hand, there is a possibility of epitaxial growth of the films. However, taking account of the lattice parameter ($d_{Pt} > d_{Ir} > d_{Ni}$), increase in Ir content should be advantageous for the epitaxial growth. Otherwise, it was mentioned that the preferred orientation of the electrodeposited alloys depended on the different overvoltage (η) in the cathode.[19] At low overvoltage, the grains usually grow perpendicularly to the highest density planes. When the overvoltage exceeds a critical value, other directions may become the preferred orientation. The formation of films with ⟨200⟩ preferred orientation can be due to the relatively high overvoltage. To measure the overvoltage should be our future work.

3.4 Effects of pre-deposition

In this study, Pt and Ni layers were respectively pre-deposited on the substrates before electroplating Pt–Ir films. Figure 4 shows the change in cross-sectional morphologies and corresponding concentration profiles of (a) Pt–Ir, (b) Pt/Pt–Ir and (c) Ni/Pt–Ir coated specimens. Hereafter, they are denoted as Pt–Ir, Pt/Pt–Ir and Ni/Pt–Ir, respectively. In all the cases, Pt–Ir electroplating was conducted at the same current density (0.55 A/dm^2) and Ir ion mole fraction (0.95). Deposition times of Pt–Ir, Pt/Pt–Ir and Ni/Pt–Ir were 2.5, 1.5 and 1 h, respectively.

It is found that pre-electroplating affected deposition rate and Ir-content of the Pt–Ir layer. Since the thickness of Pt–Ir layers in Fig. 4 are almost identical, it is concluded that the highest deposition rate was obtained in Ni/Pt–Ir, followed by Pt/Pt–Ir and Pt–Ir had the lowest deposition rate. It should

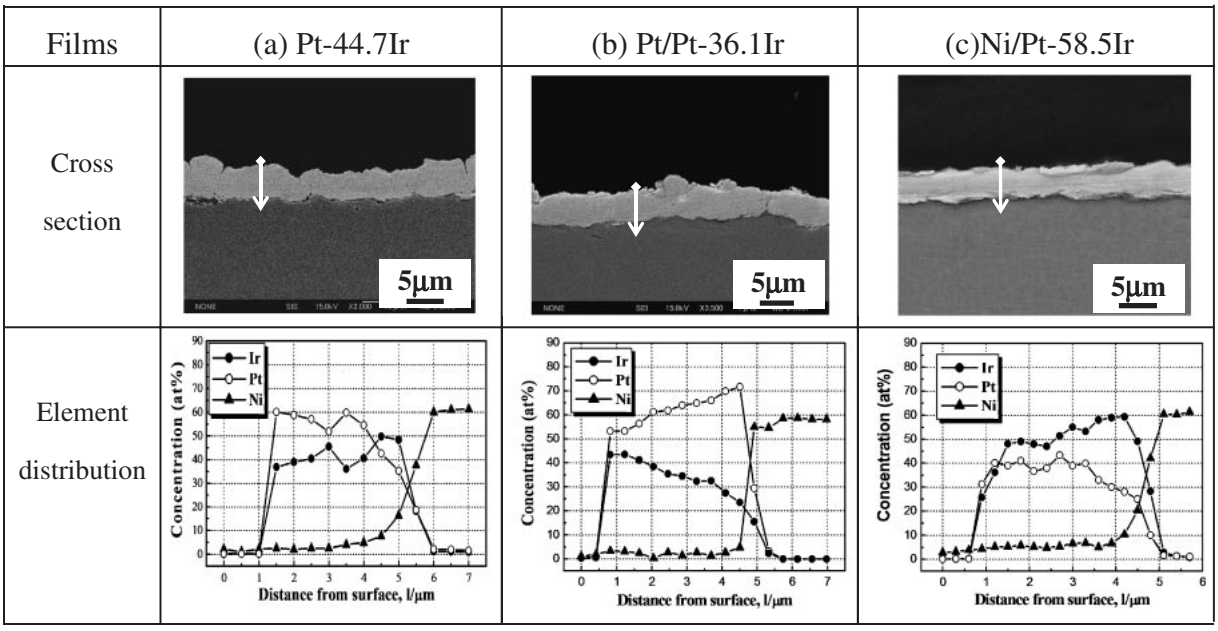

Fig. 4 Cross-sectional morphologies and corresponding concentration profiles of (a) Pt–44.7Ir, (b) Pt/Pt–36.1Ir and (c) Ni/Pt–58.5Ir coated TMS-82+ (electroplating conditions for Pt–Ir alloys: $[Ir^{3+}]/([PtCl_6^{2-}] + [Ir^{3+}])$: 0.95; current density: 0.55 A/dm^2; deposition time: (a) 2.5 h, (b) 1.5 h, (c) 1 h).

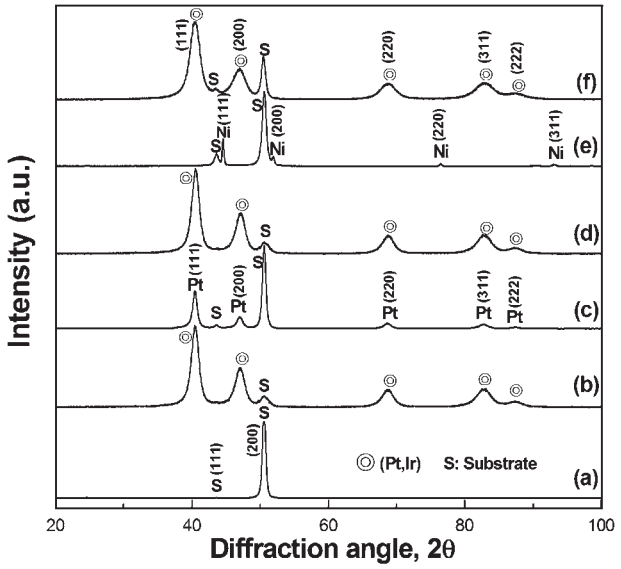

Fig. 5 X-ray diffraction patterns of (a) substrate, (b) Pt–44.7Ir, (c) pre-deposited Pt, (d) Pt/Pt–36.1Ir, (e) pre-deposited Ni and (f) Ni/Pt–58.5Ir (electroplating conditions for Pt–Ir alloys were shown in Fig. 4).

also be noted that Ni/Pt–Ir contained highest Ir content (58.5 at% on average), in which Ir concentration gradually decreased with deposition time. Pt–Ir (44.7 at%) had similar tendency whereas Pt/Pt–Ir contained only 36.1 at% Ir, and Ir concentration increased with deposition time.

These differences in composition and deposition rate of electroplated Pt–Ir films can be explained by the lattice parameter and crystal orientation of the surface on which Pt–Ir electroplating is conducted. As described in Section 3.3, the Pt–Ir films exhibited the ⟨111⟩ preferred growth orientation when Ir content exceeded 3 at%. While the Ni-base single crystal superalloy substrate is oriented along ⟨200⟩ direction, pre-deposited Ni and Pt surfaces were both oriented along ⟨111⟩, as shown in Fig. 5. The Pt–Ir layer having a preference to ⟨111⟩ growth orientation can be more easily deposited on {111} surfaces than on {200}. It is thus concluded that increase in deposition rate by the pre-deposition of Ni and Pt can be caused by the change of surface orientation.

Once the ⟨111⟩ oriented surface is formed, the overlaying layer tend to decrease the interface energy, thus reducing the lattice misfit at the interface. Since the lattice parameter is smallest in Ni and largest in Pt ($d_{Ni} < d_{sub} < d_{Ir} < d_{Pt}$), the pre-deposited Ni surface can give rise to the preferential deposition of Ir, while Pt enhances the preferential deposition of Pt. The ⟨111⟩ oriented Ni pre-deposition is therefore effective in increasing the Ir content in co-electroplating of Pt–Ir system. To electroplate Pt–Ir alloys on the {111} surface of Ni-base single crystal superalloy substrate is interesting because it should enhance the deposition rate and also increase Ir-content in the deposits. This work should be done and will be reported near future.

4. Conclusions

Pt–Ir (Ir $\leqslant$ 58.5 at%) alloys were electroplated on the Ni-base single crystal superalloy, with the thickness of 3–5 μm. The results are summarized as follows.

(1) Electroplating of Pt–Ir alloys from the amidosulfuric acid electrolytes exhibited a preferential deposition of Pt.
(2) The surface of Pt–Ir films was granular consisting of numerous nodules whose mean size increased with deposition time and current density.
(3) An fcc single phase was formed, in which the preferred orientation was ⟨111⟩, except for the Pt–2.9Ir film.
(4) Pre-deposited Ni surface gave rise to the preferential deposition of Ir while Pt enhanced the preferential deposition of Pt. Both of them increased the deposition rate of Pt–Ir alloys by the change of surface orientation.

REFERENCES

1) T. Cape: U.S. Patent 3,102,004 (1963).
2) K. Bungardt, G. Lehnert and H. Meinhardt: German Patent 1,796,175 (1971).
3) E. C. Duderstadt and A. N. Bangalore: U.S. Patent 5,238,752 (1993).
4) J. H. Chen and J. A. Little: Surf. Coat. Technol. **92** (1997) 69–77.
5) H. M. Tawancy, N. Sridhar, B. S. Tawabini, N. M. Abbas and T. N. Rhys-Jones: J. Mater. Sci. **27** (1992) 6463–6474.
6) W. T. Wu, A. Rahmel and M. Schorr: Oxid. Met. **22** (1984) 59–81.
7) D. He, H. Guan, X. Sun and X. Jiang: Thin Solid Films **376** (2000) 144–151.
8) T. E. Strangman and P. A. Solfest: U.S. Patent 4,880,614 (1989).
9) H. Murakami, T. Yano and S. Sodeoka: Mater. Trans. **45** (2004) 2886–2890.
10) E. P. George and C. T. Liu: *Micro- and Macro-Alloying of Ir Base Alloys*, (E. K. Ohriner *et al.* (Eds.), Iridium, The Minerals, Metals and Materials Society, Warandale, 2000) pp. 3–14.
11) W. M. Clift, K. F. McCarty and D. R. Boehme: Surf. Coat. Technol. **42** (1990) 29–40.
12) P. Kuppusami and H. Murakami: Surf. Coat. Technol. **186** (2004) 377–388.
13) F. Wu, H. Murakami and H. Harada: Mater. Trans. **44** (2003) 1675–1678.
14) F. Wu, H. Murakami and A. Suzuki: Surf. Coat. Technol. **168** (2003) 62–69.
15) F. Wu, H. Murakami, Y. Yamabe-Mitarai, H. Harada, H. Katayama and Y. Yamamoto: Surf. Coat. Technol. **184** (2004) 24–30.
16) G. A. Conn: Plating **52** (1965) 1258–1261.
17) T. B. Massalski: *Binary Alloy Phase Diagrams*, (ASM International, 1990) pp. 1427.
18) D. B. Knorr and D. P. Tracy: Appl. Phys. Lett. **59** (1991) 3241–3243.
19) Z. X. Huang and C. S. Wu: *Electroplating Theory*, (Science and Technology Press, Beijing, 1982) pp. 86.